energies

MDPI

Article

Study on Unblocking and Permeability Enhancement Technology with Rotary Water Jet for Low Recharge Efficiency Wells in Sandstone Geothermal Reservoirs

Chao Yu [1], Tian Tian [2], Chengyu Hui [1], Haochen Huang [1] and Yiqun Zhang [1,*]

[1] State Key Laboratory of Petroleum Resources and Prospecting, China University of Petroleum-Beijing, Beijing 102249, China
[2] Engineering Research Institute, Sinopec Shanghai Offshore Oil & Gas Company, Shanghai 200120, China
* Correspondence: zhangyq@cup.edu.cn

Abstract: In China, sandstone geothermal reservoirs are large in scale and widely distributed, but their exploitation is hindered by low recharge efficiency. In this paper, an unblocking and permeability enhancement technology using a rotary water jet for low recharge efficiency wells in sandstone geothermal reservoirs is proposed to solve this problem. This paper presents a series of studies about the proposed technology, including experiments, simulation and field application. Firstly, an experiment was carried out to verify the scale removal effect of a high-pressure water jet on the inner wall of the screen tube and its impact on sandstone. Secondly, the numerical models of the rotary jet flow field in the wellbore were established by ANSYS Fluent to study the influence of parameters. Finally, based on the simulation and experiment results, a rotary jet tool applicable to unblocking and descaling low-efficiency wells was designed, and a field application for low-efficiency wells in sandstone thermal reservoirs was conducted. The study results show that the unblocking and permeability enhancement technology using a rotary water jet is effective in removing the blockages and improving the permeability near the well. In conclusion, the presented technology can solve the problem of low efficiency during the reinjection of cooled thermal waters back into sandstone geothermal reservoirs and has great effectiveness in field application.

Keywords: sandstone reservoir; rotary jet; recharge efficiency; unblocking; permeability enhancement

Citation: Yu, C.; Tian, T.; Hui, C.; Huang, H.; Zhang, Y. Study on Unblocking and Permeability Enhancement Technology with Rotary Water Jet for Low Recharge Efficiency Wells in Sandstone Geothermal Reservoirs. *Energies* **2022**, *15*, 9407. https://doi.org/10.3390/en15249407

Academic Editor: Reza Rezaee

Received: 2 November 2022
Accepted: 6 December 2022
Published: 12 December 2022

1. Introduction

Geothermal energy is a non-polluting renewable energy source compared to traditional fossil energy sources, which has the advantages of local access, stable operation and clean environmental protection [1,2]. Geothermal resources mainly comprise hot dry rock and hydrothermal resources, the latter requiring less technical requirements and being more economical to develop [3–5]. China's sandstone geothermal resources have an abundant, widely distributed and high development potential, which has gradually increased in development scale in recent years [6]. Utilization of geothermal fluids is a common method of hydrothermal resource development, but this method may result in different potential geological risks, such as lowering the groundwater table and ground subsidence [7,8]. Reinjection of cooled geothermal water back into the reservoir is one of the solutions [9,10]. Suspended particles in the fluid accumulate in the seepage channels during reinjection and form blockages near the wellbore, reducing the permeability of the near-well zone and ultimately causing a decrease in reinjection volume or an increase in rejection pressure in the development well [11].

Physical, chemical or biological plugs can occur during geothermal tailwater reinjection in different combinations. Physical plugs during geothermal tailwater reinjection are mainly blockages caused by suspended matter, particle transport and clay swelling. When the rechargeable geothermal reservoir is characterized by high ground pressure,

loose cementation, high clay content, low permeability and poor water circulation, these physical plugs are likely to occur [12,13]. During the reuse of geothermal water, the high concentration of chemical ions such as chloride ion and sulfate ion in the water can corrode the metal casing or screen pipe and produce insoluble substances during the reinjection process to form a chemical plug in the underground reservoir [14,15]. Microbial blockage of recharge reservoirs involves both microbiological and biochemical mechanisms of action, including colonization by the bacteria themselves and extracellular polymers, and may result in permanent blockage [16,17].

Reasonable development and utilization of geothermal energy are of great significance for reducing carbon emissions and optimizing the energy structure. The effective development and utilization of hydrothermal geothermal resources cannot be achieved without the development of unblocking technology. The velocity distribution of the swirling jet is helical, which can significantly enhance the turbulence pulsation and is conducive to flushing the attached blockage particles [18]. Cavitation occurs in the process of plug removal by rotary jet, which can clean the blockage in the seepage hole throat [19]. Based on the reservoir characteristics of sandstone thermal reservoirs and the mechanism of the rotary jet [20–22], this paper proposes a rotary jet unblocking technology applicable to low-efficiency wells [23,24]. Through laboratory experiments and numerical simulations, the author verified the effectiveness of high-pressure jet descaling and unblocking and proposed construction recommendations in sandstone geothermal reservoir infiltration enhancement operations. After field operations, the reinjection level and well conditions of the sandstone geothermal reservoir inefficient well were effectively improved. This paper provides a theoretical basis and experimental reference for the unblocking and permeability enhancement of sandstone geothermal reservoirs based on rotary jet technology and provides reference and guidance for the application and promotion of rotary jet unblocking technology in sandstone geothermal reservoirs.

2. Experiment of the Jet Pressure Wave Transmission Efficiency

In this paper, the high-pressure water jet was applied for plug removal and permeability enhancement. An experiment on the transmission efficiency of jet pressure waves was carried out to verify the scale removal effect of a high-pressure water jet on the inner wall of the screen tube and its impact on sandstone. In order to realize this experiment, different types of sandstone rock samples were attached to the outer wall of the screen tube section and were washed through a high-pressure water jet, which is used to simulate the plug removal and jetting operation in practical application.

2.1. Experiment Principle

Previous scholars have conducted many studies on the plug removal principle of sandstone reservoirs and jet impact pressure [25–27]. In this paper, an experiment was carried out to obtain high-pressure water jet pressure wave transmission efficiency for screen tubes taken from low-efficiency reinjection wells in a sandstone thermal reservoir. The layout of the experiment device is shown in Figure 1.

As shown in Figure 1, the sandstone rock sample should be cut into an arc along the outer wall of the screen tube, and the sample and the screen tube should be fitted on the experiment platform before the experiment. The jet spray gun is placed inside the cut screen tube, and the inner wall of the screen tube is continuously flushed for a period of time by a high-pressure jet according to a certain pressure and volume flow. After jet flushing, the descaling effect of the water jet on the inner wall of the screen tube, the erosion and crushing effect on sandstone samples will be observed. Thus, it can be judged whether the high-pressure water jet can continue to erode and break the sandstone samples outside the screen tube after passing through the screen tube wall and maintaining a certain jet energy.

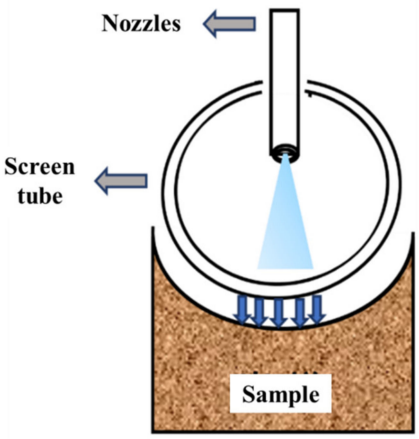

Figure 1. Experiment principal diagram.

2.2. Experiment Equipment and Materials

This experiment adopted a jet spray gun, whose structure is shown in Figure 2. In this experiment, the spray gun was equipped with three nozzles of 4.0 mm diameter. During the experiment, the screen tube could be sprayed at a fixed point, and the efficiency of the jet passing through the screen tube was studied. The experiment pump is a skid-mounted high-pressure three-cylinder plunger pump with a maximum volume flow of 0.7 m^3/min and a maximum pump pressure of 70 MPa.

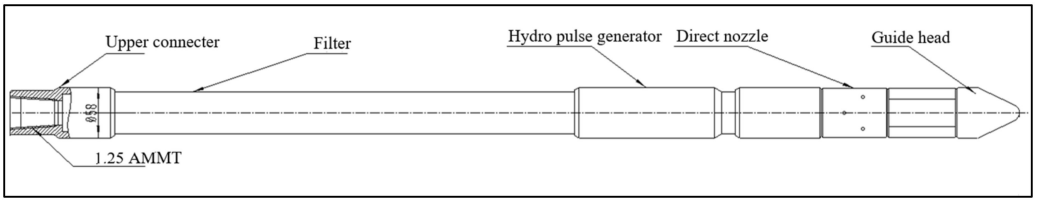

Figure 2. Schematic diagram of jet tool structure.

The screen tube used in the experiment is the wire wound screen tube used in the geothermal reinjection well of Guantao Formation in Lankao County, Henan Province. The screen tube had serious rust inside the base tube, and there was a blockage between the screen and the wire wound. Before the experiment, the reasons for the blockage of the screen tube were analyzed. As we know, the geothermal water of the Guantao Formation contains more minerals, and minerals in the geothermal water may be separated when the occurrence environment (temperature, pressure, PH value, etc.) of the local layer water changes, which form blockages and block the screen tubes and pore channels. Additionally, in the long-term injection production process, the sand production of the reservoir and the insoluble particles in the reinjection fluid also form sediment in the screen tube to block the screen tube channel, which is also the main reason for screen tube blockage. In addition, the screen tube can also be blocked by rust and sediment blockage formed by inorganic scale due to screen tube corrosion. The screen tube and inner wall used in the experiment are shown in Figure 3.

In the experiment of the jet pressure wave transmission efficiency, a yellow sandstone sample with a specification of 100 × 100 × 100 mm was adopted as the experiment rock sample. The physical parameters of the yellow sandstone type are shown in Table 1. In this experiment, the surface of the yellow sandstone rock sample was cut into an arc matching the outer wall of the screen tube to simulate the working conditions during downhole operation, which can represent the sandstone outside the well wall during the blockage removal operation to some extent. After the jet experiment, we observed whether the yellow sandstone was broken and eroded under the action of the jet to judge the efficiency of the water jet passing through the screen tube. The sandstone sample is shown in Figure 4.

Figure 3. Experiment screen tube and internal conditions.

Table 1. Physical parameters of yellow sandstone for experiment.

Parameter	Unit	Value
Density	g/cm^3	2.52
Uniaxial compressive strength	MPa	99.771
Elastic modulus	GPa	24.2
Poisson's ratio	/	0.182
Permeability	mD	0.0184
Porosity	%	4.33

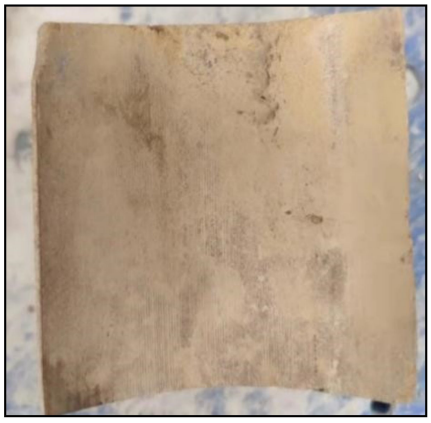

Figure 4. The yellow sandstone samples for experiment.

2.3. Experiment Scheme and Procedures

The purpose of this experiment was mainly to study whether the high-pressure water jet can effectively remove the scaling and blocking state of the screen tube. After the jet passes through the screen tube, it can achieve a certain erosion and crushing effect on the sandstone rock sample on the outer wall of the screen tube and provides a reference and basis for the on-site rotary jet unblocking operation. For this reason, an experimental scheme for the experiment of jet pressure wave transmission efficiency was designed in this section. In order to make the experiment results as close as possible to the working conditions of the on-site unblocking operation, the experiment pump pressure was set to 26 MPa, and the spray distance was set to 5.0 mm. The experiment device is shown in Figure 5.

Figure 5. Experiment device fixed.

The specific steps for the experiment are as follows:

(1) Connect the jet tools and pipelines to the skid-mounted pump and then start the pump. Run under low pressure for a period of time to test the connectivity and sealing of the experimental device, and stop the pump after the test result is stable.

(2) Cut the screen tube into sections with a length of 0.5 m, and then fix the tube sections and sandstone rock sample on the experiment platform according to the designed experiment plan. At the same time, the screen tube shall be well supported to prevent the damage of sandstone samples caused by the self-weight of the screen tube from interfering with the test results.

(3) Connect the jet tools to the centralizer, place it in the screen tube and fix it. Fix the high-pressure flexible pipe on the experiment platform to prevent shaking during the experiment.

(4) Start the skid-mounted pump. Increase the pump speed gradually when the pressure of the skid-mounted pump is stable, then raise the pump pressure to the target pressure. Record the experimental data (volume flow, pump pressure and injection time), and evaluate the injection effect during the jet experiment

(5) After the experiment, reduce the speed and gear of the skid-mounted pump gradually and stop the pump when the pressure is stable. Then remove the pipeline and screen tube, and return the test device to its original position.

2.4. Experiment Results and Analysis

During the experiment, the pump pressure was maintained at about 26 MPa, and the volume flow was maintained at 0.56 m^3/min. The spraying effect of the high-pressure jet during the experiment and the scale removal results of the high-pressure jet are shown in Figure 6.

In the process of the experiment, a large amount of water was sprayed out through the screen tube within a short time after the jet started and the pump pressure was stable. During the experiment, the high-pressure water jet could keep on spraying to the highest position of about 2 m after it quickly passed through the screen tube, the internal screen and the winding wire. The experiment lasted for 5 min.

Figure 6. Experiment flushing process.

After the experiment, the jet spray gun was taken out, and the situation of the inner wall of the screen tube after continuous flushing by a high-pressure jet was observed. The results are shown in Figure 7. It can be seen that the rust of the inner wall of the screen tube after the experiment has been significantly improved under the action of the jet, and the scaling and blockage in the inner base tube hole have also been cleaned under the action of the jet. However, the high-pressure water jet did not damage the screen between the base pipe and the winding wire, and the clogging state of the screen mesh was also significantly improved. From the flushing results of the screen tube, it can be concluded that the high-pressure water jet can produce a more effective cleaning and descaling effect on the screen tube and the internal screen without damaging them, and after passing through the screen, the energy of the water jet can still be kept at a high level. The internal condition of the screen pipe after flushing is shown in Figure 7.

Figure 7. Interior of the screen tube and the screen after the experiment.

The screen tube and sandstone sample were separated after the jet experiment. The surface morphology of the yellow sandstone sample after jet spraying is shown in Figure 8. It is obvious that after continuous washing with a high-pressure water jet, there are many erosions shallow pits on the surface of the sandstone sample at the corresponding position of the jet, and the corners are also broken under the action of the jet. It can be seen that high-pressure jet has played a certain role in the erosion and destruction of sandstone samples after passing through the screen tube. In order to further study the erosion effect of a high-pressure water jet on sandstone, the yellow sandstone samples before and after the experiment were scanned through a three-dimensional surface appearance instrument.

Figure 8. Post-experimental yellow sandstone rock sample.

The three-dimensional surface appearance instrument used was provided by our laboratory, which can scan the strength and surface height of the target rock sample without damaging the rock sample. The appearance instrument scanning device is shown in Figure 9.

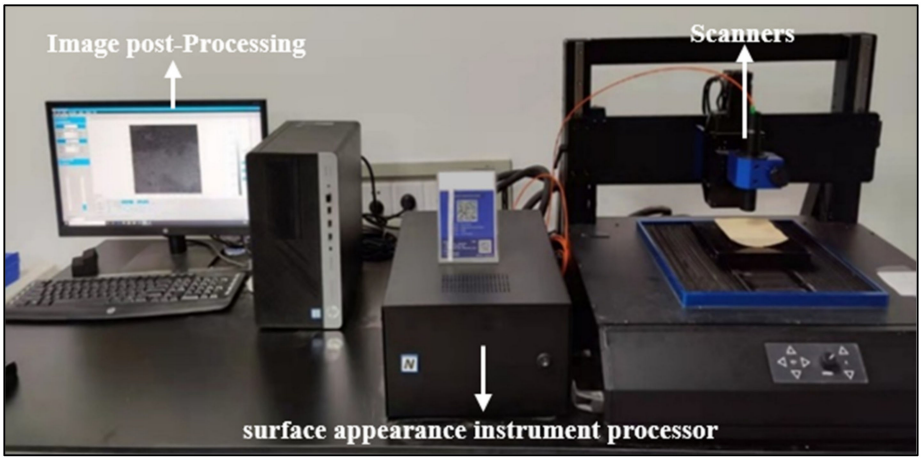

Figure 9. Three-dimensional surface appearance instrument.

The yellow sandstone samples before and after the experiment were scanned, and the scanning results are shown in Figure 10. By comparing the scanning results before and after the experiment, from the perspective of the scanning results of surface height, it can be seen that the erosion of shallow pits on the surface of the yellow sandstone rock sample after the flushing is also reflected in the scanning results. By comparing the surface strength of the yellow sandstone samples before and after the experiment, it can be seen that the overall strength of the sandstone sample surface also decreases after the high-pressure water jet flushing.

Based on the above results, it can be seen that a high-pressure water jet can play a certain role in removing the rust and scale on the inner wall of the screen pipe. The high-pressure jet can effectively pass through the screen tube wall, causing certain erosion, crushing and loosening effects on the sandstone samples on the outer wall without destroying the screen.

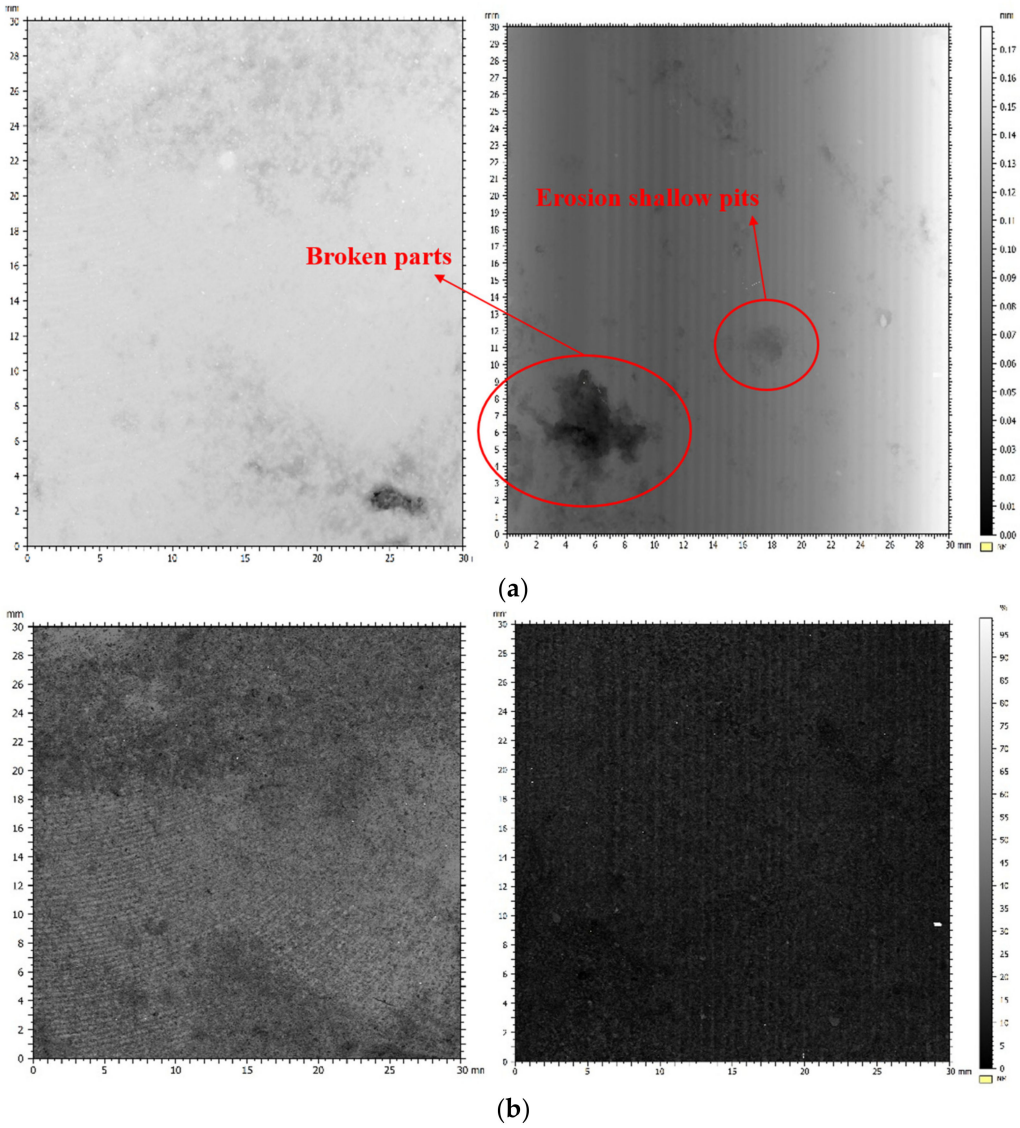

Figure 10. The scanning results of the three-dimensional appearance instrument before and after the experiment should be listed as follows: (**a**) the surface height scanning results before and after washing (**left**: before experiment; **right**: after experiment); (**b**) the surface intensity scanning results before and after washing (**left**: before experiment; **right**: after experiment).

3. Simulation Study of Rotary Jet Wellbore Flow Field

3.1. Model Description

In the process of unblocking and scale removal by rotary jet, the effect of rotary jet on the wellbore directly affects the final effect of unblocking and scale removal, and controlling the spray distance and volume flow of rotary jet tools plays an important role in the effect of the jet. In order to study the flow field characteristics and flushing range of the rotary jet in the wellbore, the flow field of the rotary jet in the wellbore was simulated using Fluent. The Eulerian multiphase model was selected, which allowed multiple independent but interacting phases to be modeled. The geometric model (Figure 11) is divided into casing area, rotation area, nozzle model and tubing area. The main setup area of the model is shown below, where the nozzle arrangement includes 1 forward nozzle, 2 inclined nozzles and 4 lateral nozzles. The model uses a 90 mm smooth cylinder to represent the wellbore, and the maximum outer diameter of the spray gun body is 30 mm. During the numerical simulation, the smooth cylinder used to simulate the wellbore remains stationary, the rotary tool rotates in the wellbore at a predetermined speed, and a rotary jet is formed in the

wellbore to act on the inner wall of the wellbore. The diameter of nozzles is 3 mm, the volume flow is 1 m^3/min and the rotational speed is 100 rpm. In this study, we set the nozzle face on the tool as the velocity inlet, and the outlet is the annular section between the well wall and the tool tubing column, which is also set as the pressure outlet, and the well wall face is set as the wall type.

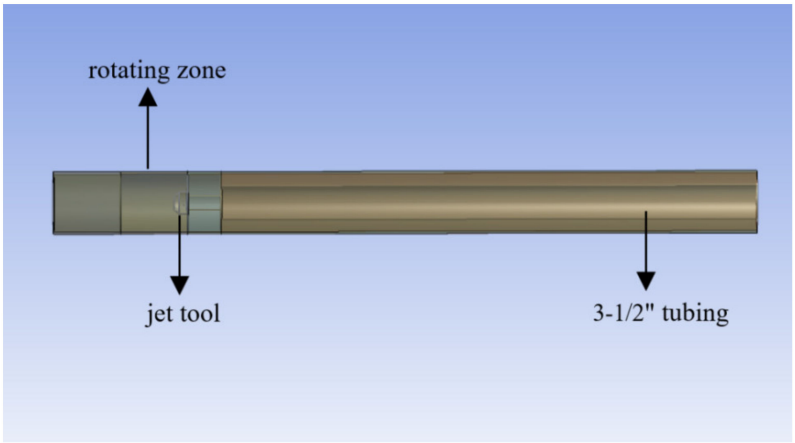

Figure 11. The diagram of the established model.

3.2. Governing Equations

In this study, the VOF model was used for the multiphase flow model in order to approximate the flow characteristics of the rotating jet in the wellbore under realistic conditions. The VOF model is a surface tracking method under a fixed Eulerian grid. In the VOF model, each fluid phase shares a common set of momentum equations, and each phase interface is tracked by introducing this variable of phase volume fraction. When we assume that the volume fraction of the q-th phase in the VOF model is α_q, then we can derive three cases: ① $\alpha_q = 0$, at which time we can know that there is no q-th phase fluid in the model cell; ② $0 < \alpha_q < 1$, at which time we can assume that the model cell contains multiphase fluid including qth phase; and ③ $\alpha_q = 1$, at which time we can assume that the model cell is filled with q-th phase fluid. The continuity equation and momentum equation of the VOF multiphase flow model are as follows.

$$\frac{\partial \alpha q}{\partial t} + \vec{v} \cdot \nabla a_q = \frac{s_{\alpha q}}{\rho_q} \tag{1}$$

In the continuity equation, $S_{\alpha q}$ is the mass source term, which is zero by default, and the volume fraction of each phase in the model is constrained to behave as follows:

$$\sum_{q=1}^{n} \alpha_q = 1 \tag{2}$$

$$\frac{\partial}{\partial t}\left(\rho \vec{v}\right) + \nabla\left(\rho \vec{v}\vec{v}\right) = \nabla p + \nabla\left[\mu\left(\nabla \vec{v} + \nabla \vec{v^T}\right)\right] + \rho \vec{g} + \vec{F} \tag{3}$$

where v denotes the fluid velocity, m/s; ρ denotes the density of the corresponding fluid, kg/m^3; $\vec{g}$ denotes the acceleration of gravity, m/s^2; μ denotes the viscosity of the phase fluid, N/m^3; and $\vec{F}$ denotes the interfacial force source term, N·m/s^2.

In this study, the realizable k-ε model was used for the calculation. The control equations of the k-ε model mainly include the k transport equation and the ε transport equation.

$$\frac{\partial}{\partial t}(\rho k) + \frac{\partial}{\partial x_j}\left[\left(\mu + \frac{\mu_t}{\sigma_k}\right)\frac{\partial k}{\partial x_j}\right] + G_k + G_b - \rho\varepsilon - Y_M + S_k \tag{4}$$

where k denotes the turbulent energy; μ denotes the viscosity of the fluid, N/m^3; G_k denotes the generation term of the turbulent energy k caused by the mean velocity gradient; σ_k denotes the Prandtl number corresponding to the turbulent energy k; and S_k denotes the source term.

$$\frac{\partial}{\partial t}(\rho\varepsilon) + \frac{\partial}{\partial x_j}(\rho\varepsilon\mu_j) = \frac{\partial}{\partial x_j}\left[\left(\mu + \frac{\mu_t}{\sigma_\varepsilon}\right)\frac{\partial \varepsilon}{\partial x_j}\right] + \rho C_1 S_\varepsilon - \rho C_2 \frac{\varepsilon^2}{k + \sqrt{v\varepsilon}} + C_{1\varepsilon}\frac{\varepsilon}{k}C_{3k}G_b + S_\varepsilon \quad (5)$$

$$C_1 = max\left[0.43, \frac{\eta}{\eta + 5}\right] \quad (6)$$

$$\eta = S\frac{k}{\varepsilon} \quad (7)$$

$$S = \sqrt{2S_{ij}S_{ij}} \quad (8)$$

where ε denotes the turbulent dissipation rate; σ_ε denotes the Prandtl number corresponding to the turbulent energy ε; C_1, C_2, $C_{1\varepsilon}$ and C_{3k} denote the coefficients in the equation; and S_ε denotes the source term.

3.3. Meshing Schemes

In the process of numerical simulation, the quality of grid division is very important to the results of numerical simulation. The finer the grid division, the higher the accuracy of the calculation results, but correspondingly, more calculation time is required. Therefore, in the process of numerical simulation research, it is necessary to comprehensively consider the calculation time and accuracy to reasonably divide the grid. Since the rotary jet tool rotates at a predetermined speed while the wellbore remains stationary during the rotary jet plug removal operation, the grid needs to be divided according to the model area, and the rotary area and the static area need to be divided, respectively. For areas with regular shapes, such as wellbore, we used structured grids to divide them, while for other areas, such as the nozzle, we used structured and unstructured grids to divide them. In this paper, the nozzle tool part was divided into 196,205 grids. At the same time, in order to improve the calculation accuracy of the model, we partially densified the grid at the nozzle, as shown in Figure 12.

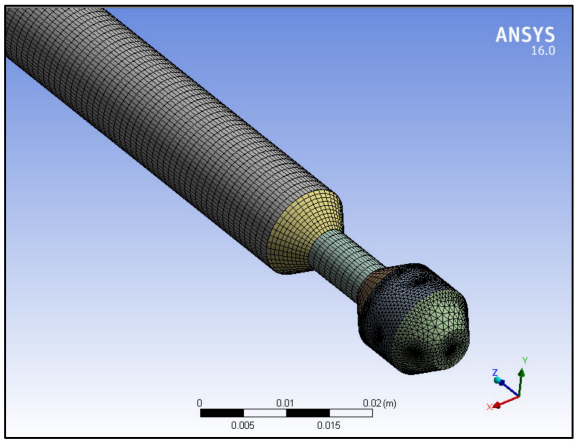

Figure 12. Meshing schemes of the established model.

3.4. Flow Field Characteristics

According to the flow field simulation results, the rotary jet could cover the whole wellbore sufficiently within a short period of time at the beginning of flushing (Figure 13). This showed that the rotary jet could fully and adequately clean the clogged and scaled locations in the wellbore with the tool in tow. By intercepting the flow field at a certain moment, it could be seen that the jet at this time has a good spot-flushing effect on the

wellbore. However, due to the effect of the jet by the forward nozzle, the energy of the jet will be lost quickly in a short distance. Therefore, in practical applications, the volume flow should be increased to some extent, the spray distance should be controlled, and the full flushing of the wellbore should be achieved by dragging the tool up and down to improve the descaling rate.

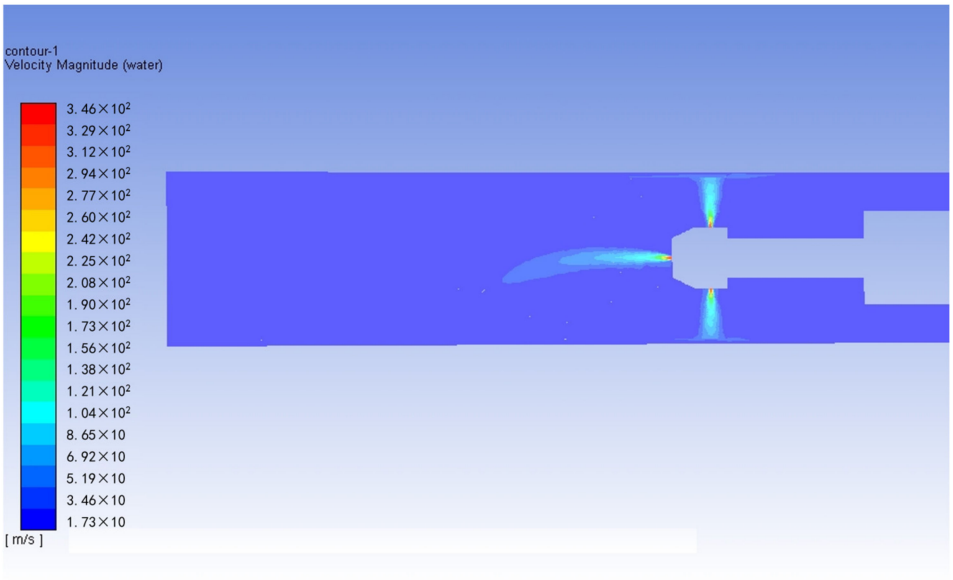

Figure 13. Schematic diagram of rotary jet's flushing effect.

In order to study the flow field distribution of the rotary jet in the wellbore, we first simulated the flow field of the rotary jet in the wellbore 1.0 s after the start of the jet, of which the results are shown in Figure 14. From the simulation results, the rotary jet has fully covered the entire wellbore within a short time of the start of the jet. Therefore, the method of dragging the rotary jet tool up and down is proposed in this paper. The method of unblocking and descaling the wellbore and near-wellbore zone through a rotary jet is practical and feasible. However, from the initial calculation example, the energy loss of the rotary jet in the wellbore is very fast. When the rotary jet reaches the wellbore, the jet velocity drops considerably, and the jet spreads gradually. It is also necessary to study the influence factors such as spray distance by changing the tool size.

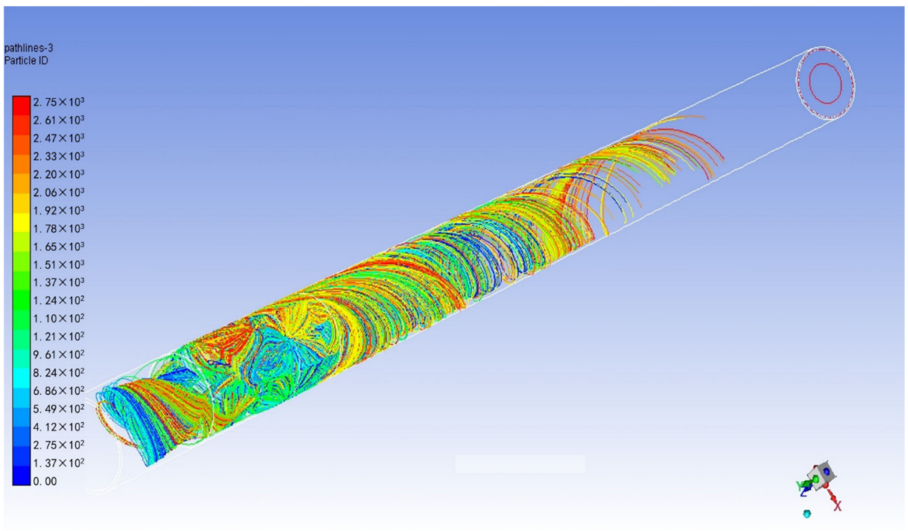

Figure 14. Schematic diagram of rotary jet's flow field.

3.5. Influence of Spray Distance

When the tool is engaged in the rotary jet unblocking operation, it needs to drive the nozzle at a certain speed and at a suitable distance to carry out jet flushing to remove the scale from the inner wall of the wellbore. From the previous numerical simulation results, it can be seen that the jet energy changes rapidly in the wellbore, which showed that the spray distance is an important factor affecting the effect of unblocking and scale removal. In order to achieve the best jet impact effect, the geometric model needs to be modified, so this section first carries out numerical simulation research around the influence of spray distance on the jet effect.

On the basis of previous studies on blockage removal and impact efficiency of the rotary jet [28,29], the spray distance is divided into 5.0 mm, 7.0 mm, 10.0 mm, 12.0 mm and 15.0 mm for research in this section. In order to study the influence of spray distance on the flow field of the rotary jet, the bottom nozzle and oblique nozzle on the rotary jet nozzle are canceled in this section to reduce the interference to the lateral rotary jet in the simulation process. The geometric model after changing the spray gun settings and spray distance is shown in Figure 15. The model area mainly includes the spray gun body, rotation area and wellbore area.

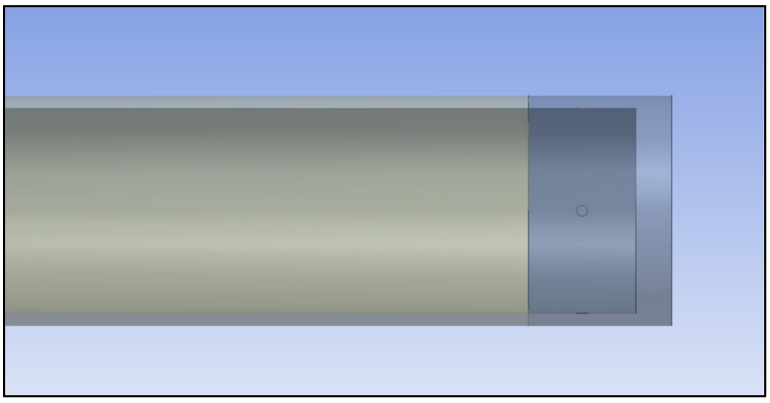

Figure 15. Schematic diagram of geometric model.

Through the simulation of the rotary jet flow field in the wellbore annulus 1.0 s after the start of the jet, it can be seen from the numerical simulation results that when the jet pitch of the rotary jet is 5.0 mm, the rotary jet can still effectively cover the wellbore area from the results of the rotary jet trajectory diagram. Therefore, we believe that when the spray distance is small, the rotary jet can still completely and fully clean the inner wall of the wellbore, making the jet less affected by interference.

During the rotary jet blockage removal operation, the distance of the rotary jet tool has an important influence on the blockage removal effect. When the distance is smaller, the energy attenuation of the high-pressure rotary jet when it contacts the inner wall of the wellbore is smaller, and the impact effect on the wellbore is stronger. At this time, the blockage removal and scale removal effect of the rotary jet is better. The influence of five groups of different jet pitches on the velocity distribution of rotary jets in the wellbore is studied by numerical simulation. The simulation results are shown in Figure 16.

From the simulation results, it can be seen from Figure 17 that when the spray distance is 5.0–10.0 mm, there is no significant difference in the flow field changes in the rotary jet in the wellbore with the increase in the spray distance. Therefore, the jet can effectively act on the inner wall of the wellbore within this range. However, when the spray distance is greater than 10.0 mm, it can be seen from the velocity distribution diagram of the rotary jet in the wellbore that the effect of the jet on the wellbore has been relatively attenuated, and the jet is relatively divergent before reaching the wellbore.

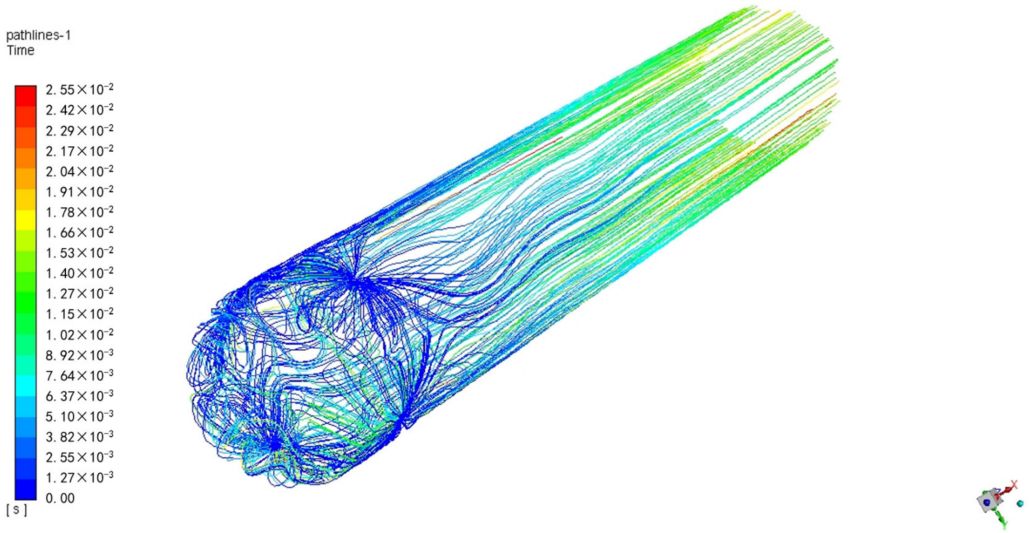

Figure 16. Trajectory map of rotary jet in the wellbore.

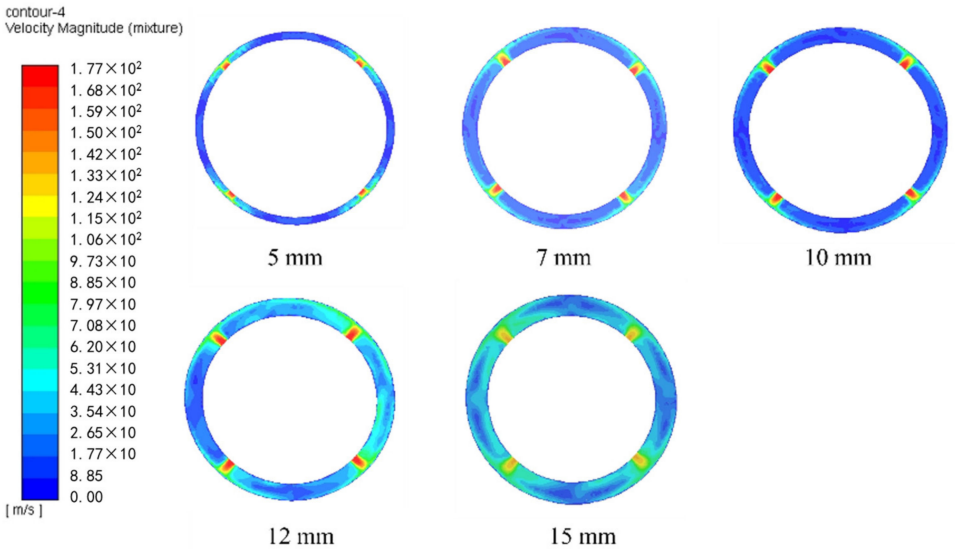

Figure 17. Velocity distribution of rotary jets at different spray distances.

Additionally, the influence of spray distances on jet pressure at the wall was studied, of which results are shown in Figure 18. It can be seen from the pressure change in the rotary jet at the well wall that the rotary jet pressure at the well wall decreases gradually with the increase in the spray distance. When the spray distance is less than 10 mm, the impact pressure of the jet on the wellbore does not drop significantly. When the spray distance is greater than 10 mm, the jet pressure at the borehole wall decreases rapidly with the increase in spray distance.

Through the analysis of the simulation results, it can be concluded that the jet energy loss will become greater with the increase in spray distance when the rotary jet reaches the inner wall of the wellbore during the plug removal operation. Therefore, during the rotary jet blockage removal operation, the jet spacing can be controlled within 5.0–10.0 mm according to the simulation results. At the same time, centralizers can be installed at the upper and lower ends of the tool string according to the actual well conditions to prevent the tool from jamming and blocking during the blockage removal operation. Reasonable jet spacing can be selected according to the actual well conditions to achieve the best blockage removal effect.

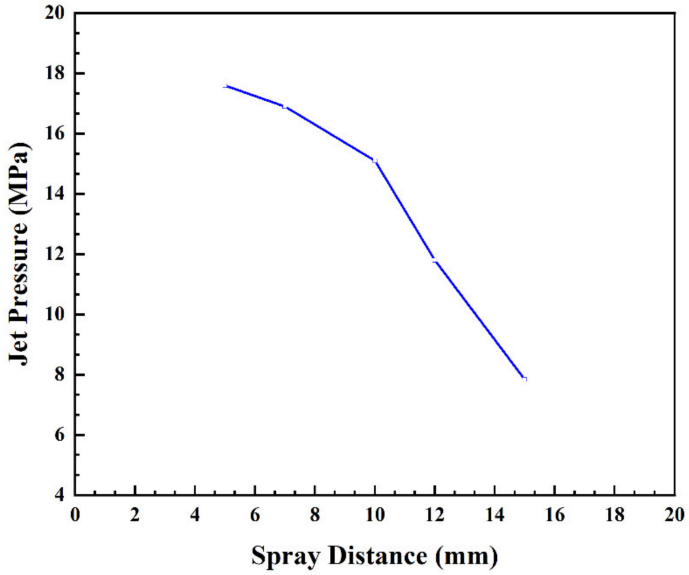

Figure 18. Variation in jet pressure at the well wall under different spray distances.

3.6. Influence of Volume Flow

During the rotary jet unblocking operation, the volume flow directly affects the jet pressure during the unblocking operation. Generally, the larger the construction volume flow is, the higher the nozzle pressure drop is, and the greater the impact of the rotary jet on the inner wall of the casing is, which has a significant impact on the unblocking operation effect. However, the more the volume flow increases, the faster the pump pressure will increase correspondingly and the higher the risk of unblocking operation. Figure 18 shows the velocity distribution law of the rotary jet in the wellbore under different volume flow rates.

It can be seen from Figure 19 that when the volume flow is less than 0.8 m^3/min, the rotary jet has little effect on flushing the inner wall of the wellbore, and most of the jet energy has been lost before reaching the wall. When the volume flow reaches 1.0 m^3/min, it can be seen that the central velocity of the rotating jet is relatively higher, which can be considered that the jet flushing efficiency is the highest at this time, and the energy loss of the jet when it contacts the inner wall is also smaller. When the volume flow continues to increase, even though the jet energy of the rotary jet is higher when it is greater than 1.0 m^3/min, the difference between the velocity distribution of the rotary jet in the wellbore and that of the rotary jet under the condition of 1.0 m^3/min is not obvious, indicating that the flushing efficiency of the rotary jet is not significantly improved at this time. In the process of rotary jet unblocking operation, with the increase in volume flow, the pump pressure also increases, bringing higher construction risks.

Additionally, the influence of volume flow on jet pressure at the wall was studied. The results are shown in Figure 20. It can be seen from the pressure change in the rotary jet at the well wall that the rotary jet pressure at the well wall increases gradually with the increase in the volume flow. When the volume flow is less than 1.0 m^3/min, it can be seen that with the increase in the volume flow, the jet pressure at the well wall increases rapidly. When the volume flow is greater than 1.0 m^3/min, the growth rate of jet pressure at the well wall decreases significantly. Combined with the flow field simulation results, we can suggest that the volume flow should be controlled at 1.0 m^3/min in the actual project.

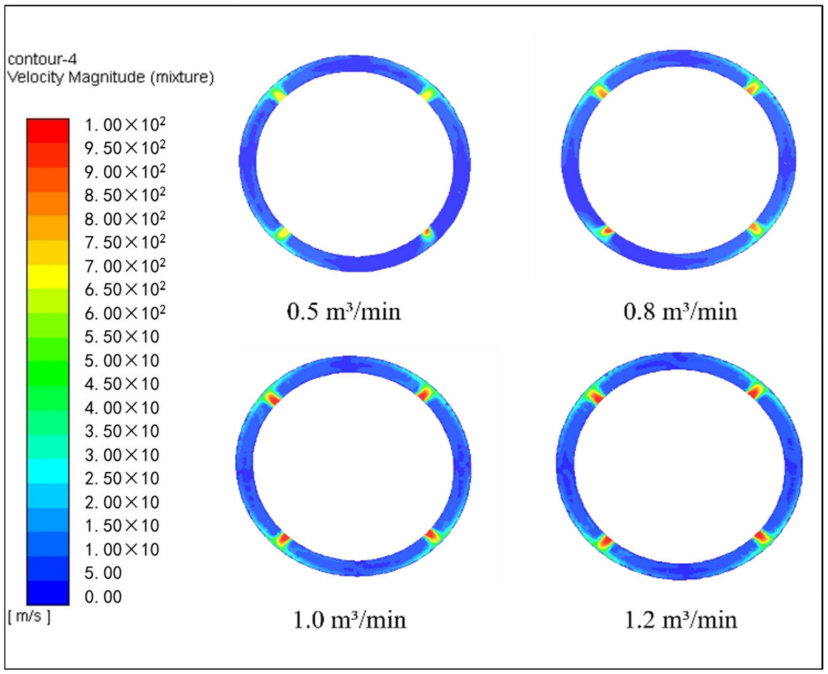

Figure 19. Velocity distribution of rotary jets at different volume flow.

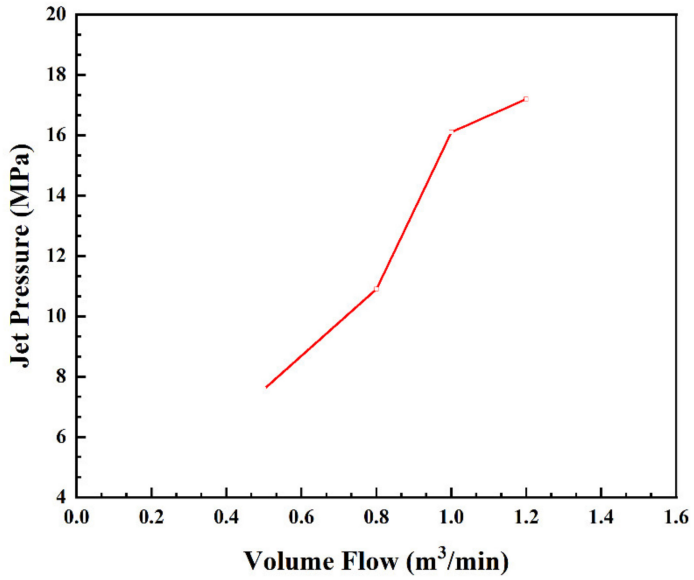

Figure 20. Variation in jet pressure at the well wall under different volume flow.

Therefore, in the actual application process, it is necessary to control the volume flow within an appropriate range to prevent high-pressure operation accidents or attenuation of volume flow from high construction pressure, which leads to the reduction in rotary jet energy, resulting in insufficient blockage removal and scale removal effect. Additionally, in order to further improve the blockage removal and scale removal effect of the rotary jet, the nozzle parameters can be designed, the appropriate nozzle combination can be used, and the operation volume flow and pressure can be appropriately increased during the blockage removal operation to achieve better blockage removal and scale removal effect.

By analyzing the change in the jet pressure at the wellbore with the spray distance and volume flow and combining it with the analysis of the flow field of the rotary jet, we can propose parameter suggestions in the actual process of the rotary jet blockage removal. Control the spray distance and volume flow in the actual operation within the appropriate range to achieve the best blockage removal effect.

4. Field Application of Rotary Jet Blockage Removal in Renre 4 Well

The aim of this section is to verify whether the high-pressure rotary water jet can effectively remove the blockage and scale of the low-efficiency wells in the sandstone thermal reservoir of the Guantao Formation and improve the permeability near the well and increase the reinjection volume. In this chapter, a low-efficiency reinjection well named Renre 4 Well, located in the Bohai Vocational College area, was selected for field application. The corresponding rotary jet unblocking construction scheme was designed, and the on-site unblocking operation was carried out. At the end of the operation, the effect of blockage removal and irrigation increase in the field application was evaluated.

4.1. Design of the Rotating Jet Unblocking Tool

In this section, based on the principle of plug removal and permeability enhancement of rotary jet for the Guantao Formation sandstone formation, combined with the results of numerical simulation and jet experiment, we designed the rotary jet plug removal tool for the problem of plug removal and permeability enhancement of low-efficiency wells in sandstone thermal reservoir, and processed the rotary jet plug removal tool for Guantao Formation sandstone thermal reservoir, providing a tool basis for on-site plug removal of the rotary jet.

The specific working principle of plug removal is as follows: before the plug removal operation, the rotary jet plug removal tool is lowered to the predetermined cleaning layer through the oil tube, and the clean water enters the jet plug removal tool through the oil tube, filter and bypass valve through the pump truck to generate multiple high-pressure water jets. At the same time, the plug removal tool nozzle is driven to rotate in the wellbore through the lifting and lowering of the string and the friction between the elastically retractable inclined roller and the inner wall of the casing. The high-pressure water jet generated by the blockage removal tool can clean the whole wellbore through direct flushing, high-frequency oscillating hydraulic wave and cavitation noise and effectively physically remove the blockage and scaling substances in the wellbore and gun hole.

The rotary jet tool has a wide range of applications. The size of the tool body and the nozzle layout of the spray gun body can be adjusted according to different working conditions and well structure. The rotary jet plug removal tool is applicable to geothermal wells or oil and gas wells where the reinjection volume is reduced due to pollution or blockage near the well zone. Geothermal wells or oil and gas wells with high formation acid sensitivity and unsuitable for acidizing and other stimulation measures. Wells have a thin reservoir and small interval, which is not easy when taking other reconstruction measures. The rotary jet tool can be used for pre-treatment before acidizing, fracturing, sand control and other measures to improve the downhole environment.

The rotary jet unblocking tool is composed of a high-pressure rotary joint, spray gun body, nozzle, rotary device, centralizer, bearing and damper. When working, the upper part of the tool is connected to the bypass valve, filter, safety connector, etc., to form a rotating jet unblocking tool string; it shall be sent to the predetermined layer for blockage removal with tubing, the ground cement truck starts the pump to pressurize, and the clean water or the working fluid added with an anti-swelling agent, wax inhibitor and clay stabilizer passes through the oil tube, filter, bypass valve (one-way valve) and then enters the incident flow unblocking tool to generate multiple radial high-pressure water jets. At the same time, the ground operation vehicle slowly lifts the tubing string to make the tool rotate while moving up and down in the cleaning section.

As the sandstone thermal reservoir of the Guantao Formation is poorly consolidated and the formation is relatively loose, Renre 4 well is completed by perforation, and the inner diameter of the casing is 226.0 mm. Therefore, to ensure the effect of blockage removal and permeability enhancement, in this chapter, in combination with the research results of numerical simulation and the experimental results of high-pressure jet blockage removal, we processed the maximum outside diameter of the rotary jet tool to 215.0 mm, and the total length of the tool was 1947.0 mm. By installing 218.0 mm centralizers at the upper

and lower ends of the tool, the rotary jet unblocking tool can ensure that the spray distance of the rotary jet nozzle can be kept within the range of 5.0–10.0 mm during the unblocking operation so as to ensure the effect of unblocking and permeability enhancement.

In this chapter, the tool spray gun body is arranged with 12 radial nozzles, which are divided into two layers. Six nozzles are evenly distributed on the spray gun body in each layer. Different nozzle combinations can be changed according to the operation requirements. The nozzle can be replaced with a combination of 2.6 mm, 3.0 mm and 4.0 mm nozzles to improve the flushing efficiency during the unblocking operation. The total length of the plug removal tool string is 2.94 m, of which the tool body is about 1.2 m long, the maximum rigid outer diameter is 215 mm, and the maximum working pressure can reach 40 MPa. The rotary jet blockage removal tool meets the requirements of the rotary jet blockage removal operation for the low-efficiency wells of sandstone geothermal reservoirs and provides the tool conditions for the field operation of rotary jet blockage removal in this chapter.

Figure 21 shows the rotary jet plug removal tool string processed in the field plug removal research in this chapter. After installation, the rotary jet plug removal tool string consists of a centralizer, rotary device, spray gun body, rotary joint, short filter joint and safety joint. The rotary joint and short filter joint are connected by a ball socket. Before the plug removal, put the steel ball into the ball socket from the wellhead, and the safety joint is connected with a 2–7/8″ oil tube, and then put the tool into the wellhead.

Figure 21. Installation diagram of rotary jet unblock tool.

4.2. Construction Process and Parameters

In this section, we carried out the rotary jet unblocking operation of Renre 4 Well in the western region of Renqiu (Figure 22) and carried out the continuous rotary jet unblocking operation for the predetermined unblocking zone of Well Renre 4. The construction process parameters and application effects are as follows.

In the design of the rotary jet unblocking process for Renre 4 Well, the pump pressure is maintained below 25 MPa during construction, the construction volume flow is maintained at 1.2 m^3/min, the total length of the unblocking operation interval of Renre 4 Well is 334 m. During the construction process, a single oil tube is lifted and lowered three times. There are 22 unblocking intervals in the construction process, and the total duration of the unblocking operation is 5.2 h. The specific unblocking data are shown in Table 2.

Figure 22. The process of Renre 4 well unblocking operation.

Table 2. Unblocking operation parameters of Renre 4 well.

Construction Layer m	Interval Number /	Pressure MPa	Volume Flow m^3/min
1784–1931	14	18.4–20.8	1.18–1.21
1529–1716	8	18.8–21.7	1.20–1.26

4.3. Results and Analysis of Field Application

In the process of rotary jet unblocking operation of Renre 4 Well, there is less fluid returning at the wellhead at the initial stage of unblocking operation. With the unblocking operation, the fluid return gradually occurs at the wellhead, which is turbid but has less sand content. At the later stage of the plug removal operation, there is a certain amount of sand in the wellhead return fluid. During the well flushing operation, after the completion of the plug removal operation, much sand is discharged from the circulating fluid return. The fluid return and sand production are shown in the figure below. Most of the fluid return and sand production are fracturing sand used in fracturing construction; this is consistent with the blockage analysis results of Renre 4 Well in the previous study. After the blockage removal operation, the bottom hole condition and reinjection condition of Renre 4 Well were also improved significantly, as shown in Figure 23 below.

Figure 23. Returning fluid and sand output during the flushing process.

By the end of 2021, the reinjection volume of Renre 4 Well before and after plug removal was 8–9 m^3/h. The amount of reinjection has decreased to a lower level. After the rotary jet unblocking operation, the reinjection volume of Renre 4 Well can reach 14 m^3/h. When the pressure is 0.6 MPa, the reinjection volume can reach 15 m^3/h. The total amount of reinjection increased by 55.6–87.5%. At the end of construction, after the well flushing tool string is taken out, much asphaltene is attached to the tool surface, but the spray gun body and nozzle are kept intact, which proves that the rotary jet blockage removal tool meets the construction requirements of high-pressure rotary jet blockage removal. After the rotary jet blockage removal operation, the reinjection volume of Renre 4 Well was also effectively improved, which verifies the effectiveness of the rotary jet blockage removal and injection increase for the sandstone geothermal reservoir of Guantao Formation and the feasibility of the method.

5. Conclusions

The key findings of the study are as follows:

(1) Experiments on the transmission efficiency of jet pressure waves were designed to study the effects of high-pressure jets on screen pipe blockage removal and scale removal, as well as the erosion and fragmentation of sandstone samples. The experimental results of jet pressure wave transmission efficiency show that after continuous flushing by a high-pressure jet, the blockage and rusting state of the inner wall of the screen pipe has been significantly improved. Additionally, after passing through the screen pipe, the high-pressure jet has a certain erosion and crushing effect on the yellow sandstone on the outer wall of the wellbore. The feasibility of the rotating jet unblocking method is verified.

(2) The sandstone in Guantao Formation has poor consolidation and is loose and easily broken. Based on the experiment results, it is suggested that the conditions such as flow rate and spray distance should be controlled according to the actual situation of the formation in the process of rotary jet blockage removal to prevent damage and destruction of the formation near the well. At the same time, gas lift and other well flushing operations are required to fully clean the wellbore after the completion of jet flow.

(3) Based on the blockage removal principle of rotary jet, this paper conducted a numerical simulation study on the flow field of the rotary jet in the wellbore, which verifies the feasibility of blockage removal and enhanced injection of rotary jet for low-efficiency wells in sandstone geothermal reservoirs. The influence of spray distance and volume flow on the rotary jet was studied. Based on the numerical simulation results, suggestions on spray distance and volume flow parameters in the process of rotary jet blockage removal are proposed.

(4) The rotary jet unblocking tool and corresponding construction technology were designed, and the rotary jet unblocking construction scheme was prepared for Renre 4 Well. After the unblocking operation, the blockage of the target well was effectively improved, and the reinjection volume flow was increased. After analyzing the sediment by sampling the flowback liquid, the results are consistent with the previous analysis of blockage causes. After the completion of the blockage removal operation, the spray gun body and nozzle of the rotary jet plug removal worker are in good condition, which also proves that the set of rotary jet blockage removal tools can meet the blockage removal requirements of the low-efficiency wells in the geothermal reservoir of the sandstone of the Guantao Formation, providing some guidance on the application of the rotary jet technology in the blockage removal and permeability enhancement of the sandstone geothermal reservoir.

(5) In this paper, the application and promotion of rotary jet unblocking technology in sandstone geothermal reservoirs are provided. However, the rotary jet can be applied to other types of geothermal reservoirs, such as carbonate rock or other geothermal reservoirs, in future work. For example, the rotary jet blockage removal technology can adapt to the unblocking requirements of different types of geothermal reservoirs by changing the structure and combination of tool nozzles and combining different types of working fluids.

Author Contributions: Conceptualization, C.Y.; methodology, C.Y.; software, T.T.; formal analysis, C.Y., C.H. and T.T.; investigation, Y.Z.; writing—original draft preparation, C.Y.; writing—review and editing, C.Y., C.H. and H.H.; supervision, Y.Z. All authors have read and agreed to the published version of the manuscript.

Funding: This research was funded by the National Key Research and Development Program of China, grant number 2019YFB1504202.

Data Availability Statement: Not applicable.

Conflicts of Interest: The authors declare no conflict of interest.

References

1. Lund, J.W. Direct heat utilization of geothermal resources. *Renew. Energy* **1997**, *10*, 403–408. [CrossRef]
2. Fridleifsson, I.B. Geothermal energy for the benefit of the people. *Renew. Sustain. Energy Rev.* **2001**, *5*, 299–312. [CrossRef]
3. Hou, J.; Cao, M.; Liu, P. Development and utilization of geothermal energy in China: Current practices and future strategies. *Renew. Energy* **2018**, *125*, 401–412. [CrossRef]
4. Javadi, H.; Ajarostaghi, S.S.M.; Rosen, M.A.; Pourfallah, M. Performance of ground heat exchangers: A comprehensive review of recent advances. *Energy* **2019**, *178*, 207–233. [CrossRef]
5. Wang, G.; Song, X.; Shi, Y.; Zheng, R.; Li, J.; Li, Z. Production performance of a novel open loop geothermal system in a horizontal well. *Energy Convers. Manag.* **2020**, *206*, 112478. [CrossRef]
6. Junhong, A. Present situation and development prospect of geothermal tailwater reinjection technology in plateau. *China Plant Eng.* **2017**, *24*, 137–138.
7. Kaya, E.; Zarrouk, S.J.; O'Sullivan, M.J. Reinjection in geothermal fields: A review of worldwide experience. *Renew. Sustain. Energy Rev.* **2011**, *15*, 47–68. [CrossRef]
8. Song, X.; Zheng, R.; Li, G.; Shi, Y.; Wang, G.; Li, J. Heat extraction performance of a downhole coaxial heat exchanger geothermal system by considering fluid flow in the reservoir. *Geothermics* **2018**, *76*, 190–200. [CrossRef]
9. Seibt, P.; Kellner, T. Practical experience in the reinjection of cooled thermal waters back into sandstone reservoirs. *Geothermics* **2003**, *32*, 733–741. [CrossRef]
10. Ungemach, P. Reinjection of cooled geothermal brines into sandstone reservoirs. *Geothermics* **2003**, *32*, 743–761. [CrossRef]
11. Song, W.; Liu, X.; Zheng, T.; Yang, J. A review of recharge and clogging in sandstone aquifer. *Geothermics* **2020**, *87*, 101857. [CrossRef]
12. Siriwardene, N.R.; Deletic, A.; Fletcher, T. Clogging of stormwater gravel infiltration systems and filters: Insights from a laboratory study. *Water Res.* **2007**, *41*, 1433–1440. [CrossRef]
13. Ma, Z.; Hou, C.; Xi, L.; Yun, H.; Sun, C. Reinjection clogging mechanism of used geothermal water in a super-deep-porous reservoir. *Hydrogeol. Eng. Geol.* **2013**, *40*, 133–139.
14. Houben, G. Iron oxide incrustations in wells. Part 1: Genesis, mineralogy and geochemistry. *Appl. Geochem.* **2003**, *18*, 927–939. [CrossRef]
15. Liu, X.L.; Zhu, J.L. A study of clogging in geothermal reinjection wells in the Neogene sandstone aquifer. *Hydrogeol. Eng. Geol.* **2009**, *36*, 138–141.
16. Liu, G.; Wu, S.; Fan, Z.; Zhou, Z.; Xie, C.; Wu, J.; Liu, Y. Analytical Derivation on Recharge and Periodic Backwashing Process and the Variation of Recharge Pressure. *J. Jilin Univ. (Earth Sci. Ed.)* **2016**, *46*, 1799–1807.
17. Xia, L.; Zheng, X.; Shao, H.; Xin, J.; Sun, Z.; Wang, L. Effects of bacterial cells and two types of extracellular polymers on bioclogging of sand columns. *J. Hydrol.* **2016**, *535*, 293–300. [CrossRef]
18. Chen, J.; Yang, R.; Huang, Z.; Li, G.; Qin, X.; Li, J.; Wu, X. Detached eddy simulation on the structure of swirling jet flow field. *Pet. Explor. Dev.* **2022**, *49*, 806–817. [CrossRef]
19. Zhang, Y.; Wu, X.; Li, G.; Hu, X.; Hui, C.; Tan, Y.; Huang, H. Study on erosion performance of swirling cavitating jet for natural gas hydrate. *J. Cent. South Univ. (Sci. Technol.)* **2022**, *53*, 909–923.
20. Felli, M.; Falchi, M.; Pereira, J.A. Distance effect on the behavior of an impinging swirling jet by PIV and flow visualizations. *Exp. Fluids* **2010**, *48*, 197–209. [CrossRef]
21. Li, G.; Shen, Z.; Peng, Y. A theoretical study of hydraulically rotating jet nozzle. *Acta Pet. Sin.* **1995**, *16*, 148–153.
22. Bu, Y.; Wang, R.; Zhou, W. Study on flow principles of rotating jet. *Oil Drill. Prod. Technol.* **1997**, *19*, 7–10+105.
23. Li, J.B.; Li, G.S.; Huang, Z.W.; Song, X.Z.; Li, K. Flow Field Study on a New Kind Swirling Multi-orifices Nozzle. *Fluid Mach.* **2015**, *43*, 32–36+41.
24. Percin, M.; Vanierschot, M.; Van Oudheusden, B. Analysis of the pressure fields in a swirling annular jet flow. *Exp. Fluids* **2017**, *58*, 166. [CrossRef]
25. Li, J.; Li, G.; Huang, Z.; Song, X.; He, Z. Effect of confining pressure on the axial impact pressure of hydraulic jetting. *J. Exp. Fluid Mech.* **2017**, *31*, 67–72.
26. Liang, X.; Dezu, R.; Yonghao, M.; Jin, L.; Jianmin, G. Pressure loss and heat transfer characteristics experiment of swirling impinging jet with different shape nozzles. *J. Aerosp. Power* **2018**, *33*, 2678–2686.

27. Hanjie, C.; Zhenping, S.; Yuan, L.; Aibaibu, A.; Yuezhong, W.; Xiaowei, W. Numerical Simulation of Water Jet Perforation on Casing Surge Pressure. *Oil Field Equip.* **2020**, *49*, 45–48.
28. Ivanic, T.; Foucault, E.; Pecheux, J.; Gilard, V. Instabilities in coaxial rotating jets. *J. Therm. Sci.* **2000**, *9*, 322–326. [CrossRef]
29. Love, T.; McCarty, R.; Surjaatmadja, J.; Chambers, R.; Grundmann, S. Selectively placing many fractures in openhole horizontal wells improves production. *SPE Prod. Facil.* **2001**, *16*, 219–224. [CrossRef]